Biomass-derived Carbon dots and their coated surface as a potential antimicrobial agent

Biomass-derived Carbon dots and their coated surface as a potential antimicrobial agent

R. Blessy Pricilla[1], Moorthy Maruthapandi[2], Arulappan Durairaj[2], Ivo Kuritka[1], John H. T. Luong[3], Aharon Gedanken[2]

[1]*Centre of Polymer Systems, Tomas Bata University in Zlin, Tr. T. Bati 5678, Zlin 76001, Czech Republic*

[2]*Department of Chemistry, Bar-Ilan Institute for Nanotechnology and Advanced Materials, Bar-Ilan University, Ramat-Gan 52900, Israel*

[3]*School of Chemistry, University College Cork, Cork T12 YN60, Ireland*

Aharon Gedanken gedanken @ mail .biu. ac .il

Abstract

Carbon dots (CDs) with an average diameter of 6.3 nm were synthesized from the medicinal seed extract of Syzygium cumini L. using one-pot hydrothermal synthesis. The prepared CDs exhibited excitation-dependent emission characteristics with photoluminescence (PL) emission maxima at an excitation of 340 nm. The CDs at 500 pg/mL displayed antimicrobial activities against four common pathogens. Both Staphylococcus aureus and S. epidermidis were completely eradicated by CDs within 12 h, compared to 24 h for Escherichia coli and Klebsiella pneumonia. The release of various oxygen species (ROS) was postulated to play a critical role in bacterial eradication. The CDs decorated on cotton fabric by ultrasonication also displayed good antibacterial activities against the above bacteria. The finding opens a plausible use of CDs in biomedical textiles with potent antimicrobial properties against both Gram-negative and Gram-positive bacteria.

Keywords: Carbon dots, hydrothermal, antibacterial activity, textile

1 Introduction

In this era of growing infectious diseases, the lack of alternative antibacterial agents is an important cause of innumerable deaths. Infectious diseases are spread by infections caused by various pathogens such as bacteria, viruses, and parasites. Due to the misuse of antibiotics, antibiotic resistance by pathogens has raised concerns for human health [**1**]. Antibiotic resistance to pathogens has had a global impact, resulting in higher medical expenses and a decrease in the discovery and development of new antibiotics [**2**]. Different ways of treatments have been adopted to prevent the spread of pathogens such as the use of disinfectants; however, excessive use leads to some side effects [**3**]. Hence, the quest to obtain less toxic and more functional antibacterial materials is highly needed. Carbon-based materials can efficiently interact with bacteria because of their enhanced membrane permeability [**4, 5**]. Antimicrobial carbon-based nanomaterials include graphene sheets [**6**], graphene

oxide [**7**], carbon nanotubes [**8**], and CDs [**9, 10**]. CDs have then emerged with their outstanding characteristics such as ease of synthesis and modification, optical properties, biocompatibility, low cost, and sustainability. CDs are zero-dimensional luminescent nanoparticles with diameters below 10 nm [**11**]. Since their accidental discovery in 2004 [**12**], CDs have been explored widely to bring out their unexplored characteristics. They can be prepared via two approaches namely top-down and bottom-up [**13**]. The top-down approaches include laser ablation [**14**] and arc discharge [**15**] whereas the bottom-up counterparts focus on hydrothermal [**16**] and microwave methods [**17**]. The CDs obtained through these approaches consist of an sp^2/sp^3-hybridized carbon core with surface functional groups [**18**]. CDs are prepared from various precursors including natural fruits [**19**] and plants [**20**], polymers [**21**], biomass wastes [**22**], and chemical compounds [**23, 24**]. The intimate contact between CDs and microorganisms is determined by a variety of factors including their composition, size, shape, and surface chemistry, as well as their structure. The mechanisms through which CDs interact with the bacteria are mostly attributed to the release of reactive oxygen species-induced stress [**25**] and electrostatic interactions [**26**]. Some of the frequently tested bacteria by the CDs include $Escherichia\ coli$ and $Staphylococcus\ aureus$ (EC and SA) [**27, 28**]. Pristine and functionalized CDs have been used for antibacterial applications. CDs of 100 μg/mL synthesized from raw shrimp shells are effective against Gram-positive and Gram-negative bacteria [29]. CDs prepared from $C.$ sativa leaf extract and decorated with silver are 90% effective against SA and EC with a minimum inhibitory concentration (MIC) of 42 μg/mL [**30**]. CDs obtained from medicinal precursors have been given much attention for their efficacy against multidrug-resistant pathogens [**31, 32**].

Syzygium cumini $L.$ (SCL) is a natural seed that belongs to the tropical and subtropical family of Myrtaceae, commonly referred to as Indian blackberry or Jamun. These seeds with high contents of phenolic acids and flavonoids [**33**] are frequently used in biological applications due to their low cost, non-toxic properties, and healing potential. Diabetes, allergies, viral infection, inflammation, and gastric ulcers have all been successfully treated with SCL seeds. These seeds are particularly of great interest in human health because of their antibacterial, antiinflammatory, antioxidant, and antidiabetic characteristics. All these properties make it an effective candidate for antibacterial applications.

This study focuses on the synthesis of CDs from SCL seed extract by a hydrothermal procedure. The CDs are characterized and tested for their antimicrobial activities against four WHO high-priority pathogens: Escherichia coli (EC), $Klebsiella\ pneumoniae$ (KP), $Staphylococcus\ epidermidis$ (SE), and $Staphylococcus\ aureus$ (SA). Our group has conducted several studies to foster the use of CDs as a new class of antimicrobial agent [**34, 35**] including the CDs prepared from Piper betel leaves [**36**]. This study unravels that the newly synthesized CDs can inhibit the bacteria at a much lower concentration (500 μg/mL) within 12-24 h. Also, the scope of this work is extended to study SE and KP, which opens a wider scope of further studies from these CDs. Nontoxicity, absence of additional chemicals, lower minimum inhibitory concentration, and high antimicrobial activity make the newly synthesized CDs to be distinctive. Based on ultrasoni-cation, as-prepared CDs are coated onto the surface of pure cotton textiles without the use of chemicals. This procedure can be applied to textiles [**37**] and polymers [**38**] with excellent coating durability after 65 washing cycles at 75 °C [**39**].

2 Experimental section

2.1 Materials

SCL seeds collected from Tamil Nadu, India, were dried and ground with a mixer to obtain the powder. For the synthesis of CDs, ultrapure water from Alfa Aesar (Haverhill, MA, USA) was used. EC (ATCC

25,922), SA (ATCC 29,213), SE (ATCC 12,228), and KP (ATCC 700,603) were attained from Dr. Banin's Lab, The Mina and Everard Goodman Faculty of Life Science, Bar Ilan University, Israel. A commercial 100% cotton fabric was obtained from a local store.

2.2 Instrumentation

The transmission electron microscope with the model number TEM-JEOL-2100 (Peabody, MA, USA) was used to capture the image of the particle size. A few drops of the CDs solution were dropped on the copper grid and dried overnight at 60 °C. The UV-visible spectrophotometer-type Varian Cary 100 Bio Spectrophotometer was used for the absorbance studies. The emission studies were obtained using a Varian Cary Eclipse fluorescence spectrophotometer. Fourier transform infrared ($FTIR$) spectra were collected ranging from 500 to 4000 cm^{-1} from a Tensor 27 spectrometer (Bruker, Germany). The surface charge was observed on Malvern Zetasizer Nano-ZS (Malvern, UK). X-ray photoelectron spectroscopy was conducted by an XPS, Nexsaspectrometer (England). For all elements, the binding energies were set by the C1s peak at 285 eV. The reactive oxygen species (ROS) generation of CDs was recorded on a Bruker X-band spectrometer (121 EPR 100d) with $DMPO$ (5,5-dimethyl^{-1}-pyrroline-N-oxide) as a spin trap. The CDs solution (40 μL) was taken and mixed with 10 μL of $DMPO$ (0.01 M) for electron paramagnetic resonance (EPR) measurement. The blank was measured using deionized water without CDs.

2.3 Preparation of Carbon dots (CDs)

The powder of SCL (1 g) was added to 60 mL of water and subjected to stirring at 650 r/m and 90° C for 60 min. After centrifugation at 9000 r/m, the supernatant was poured into a Teflon container and incubated at 200° C for 8 h. After cooling at room temperature, a dark brown solution was obtained. The solution was then filtered using a 0.22-μM filter, followed by dialysis for 24 h. The dialyzed solution was again filtered using a 0.22-μM filter and stored in the fridge until needed.

2.4 Antibacterial activity of CDs

EC, SA, SE, and KP were grown overnight with agitation at 120 rpm in lysogeny broth (LB) at 37 °C. The bacterial concentration during incubation was analyzed by taking the absorbance or optical density (OD) at 595 nm (OD_{595}). Based on the obtained values, the bacterial concentration was adjusted to 105. For the antibacterial studies with CDs, 500 pL of CDs and 500 pL of 105 bacterial solutions were mixed and incubated at various time intervals with constant shaking at 120 r/m. The control consisted of only bacterial solution and deionized water for comparison. To observe the time-dependent activity of the CDs, 3-time intervals of 0 h,12 h, and 24 h were selected. After each time interval, an appropriate amount of the incubated sample was taken and plated in a 96-well plate and subjected to 7 dilutions. After dilution, 5 pL of each dilution was taken and plated on an agar plate and incubated at 37 °C along with the control. A similar procedure was carried out for various concentrations of the CDs for 24 h. The colony-forming unit (CFU) method was used to calculate the rate of bacterial growth observed in the agar plate.

Scheme 1 The schematic illustration of synthesis and fabrication of carbon dots/cot-ton coated with carbon dots

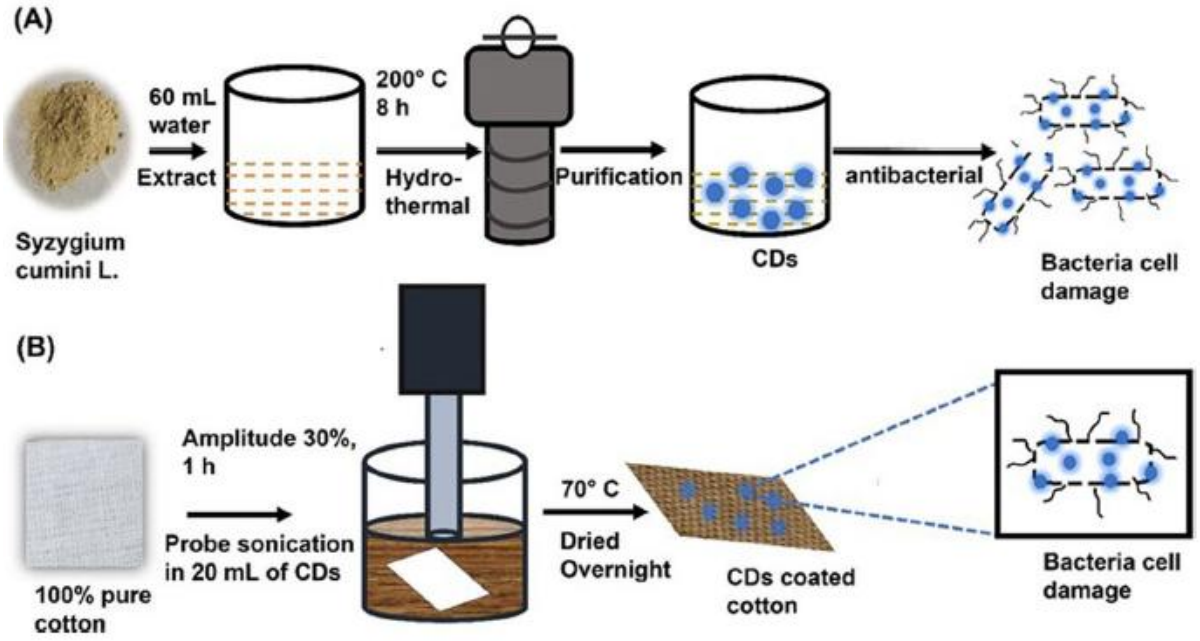

2.5 Fabric coating

For the decoration of CDs on textile, a commercial cloth (1 cm × 1 cm) with 100% cotton was submerged and sonicated in 20 mL of CDs [**40, 41**]. The probe ultrasonica-tion step was carried out for 1 h with an amplitude of 30%. The resulting cloth was dried in an oven at 70 °C overnight and used for antibacterial studies against the aforementioned bacterias. The schematic illustration is given in **Scheme 1**.

2.6 Antibacterial activity of CDs on fabric

The CDs-decorated fabric was incubated with 1 mL of bacterial suspension overnight at 37° C with constant shaking at 120 r/m. After 24 h, an appropriate amount was taken and diluted in a 96-well plate with up to 7 dilutions. From each dilution, 5 pL is taken and plated on an agar plate and incubated overnight at 37° C. The CFU method was utilized to observe bacterial growth.

3 Result and discussion

As-prepared CDs displayed a spherical shape (**Fig. 1**A) with an average diameter of 6.3 nm (**Fig. 1**B). ImageJ software was used to analyze the size of the particles. The CDs exhibited good blue luminescence with two peaks in the UV absorption spectrum **(Fig. 2**A). The peaks observed at 252 and 285 nm were attributed to the π-π^* transition of the $C = C/C = N$ bonds [**42**]. The peak around 363 nm was mainly due to the n-π^* energy transition of the $C = O$ bonds [**43**].

The CDs show excitation-dependent emission characteristics with photoluminescence (PL) emission maxima at an excitation of 340 nm (**Fig. 2**B). Among various plausible mechanisms, the most well-known ones are related to the quantum confnement efect [**44**], surface state [**45**], and molecule

fuorophore [**46**]. SCL is rich in phenolic groups and favonoids, thus, such groups should also be present on CDs [**47**].

The presence of many oxygen groups on CDs can create defects due to surface oxidation, resulting in different emission sites on their CDs and fluorescence behavior. Typically, the ability to trap excitons (i.e., electrons and holes) increases with the number of surface imperfections. Consequently, the red-shifted emission is caused by the radiation produced by the recombination of entrapped excitons. Various functional groups were observed through the $FTIR$ spectrum (**Fig. 1**C). The $FTIR$ peak observed at 3698 cm^{-1} attested to the presence of a strong OH group.

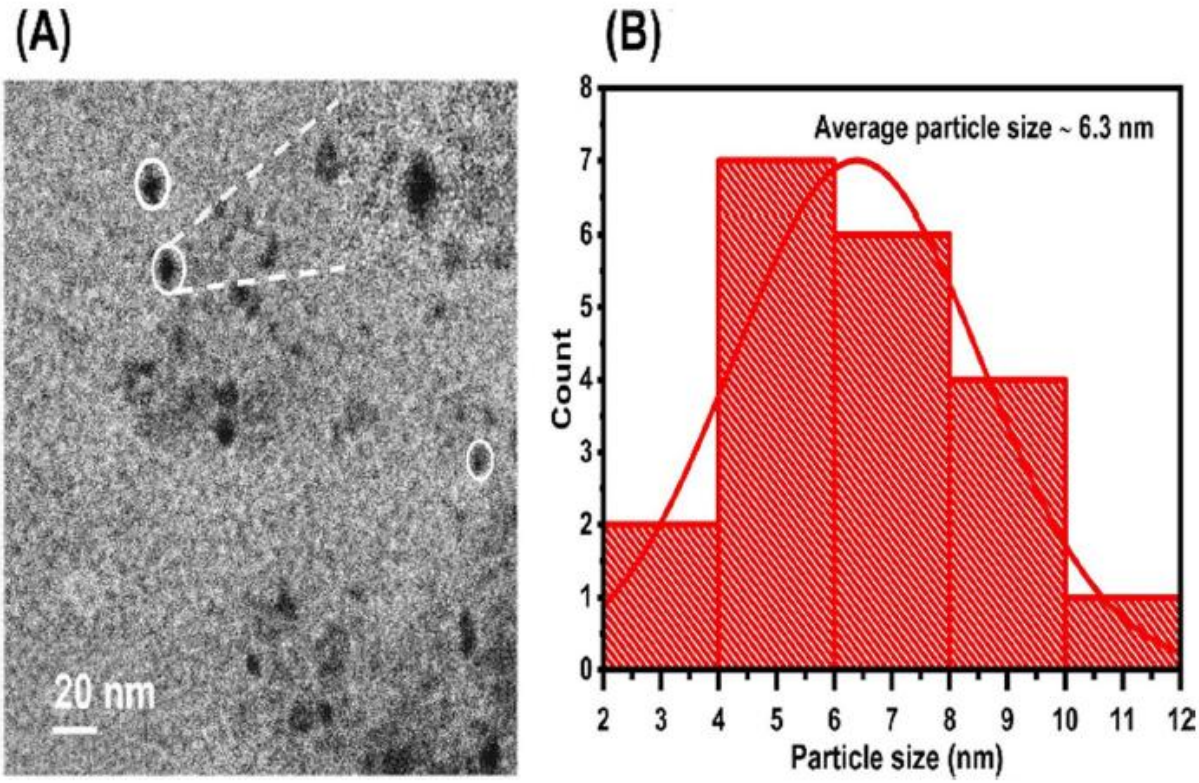

Fig. 1 A TEM image of CDs, B particle size distribution of CDs

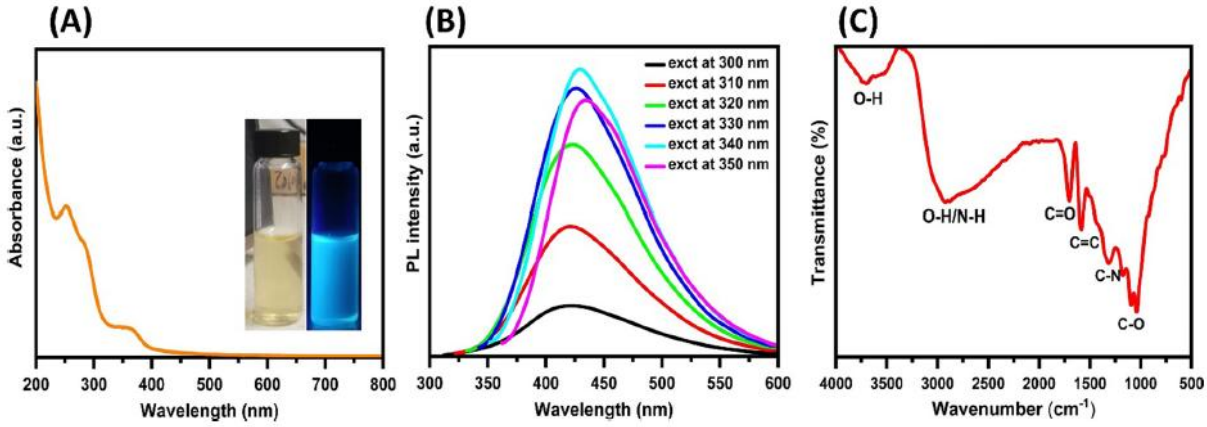

Fig. 2 A UV spectrum of CDs, B PL emission characteristics of CDs, and C $FTIR$ spectrum of the CDs

The broad peak observed from 3378 to 2159 cm^{-1} represented OH vibrations of the carboxylic acids and $N-H$ stretching vibrations. The peak around 1700 cm^{-1} was attributed to the $C = O$ stretching

of the conjugated system of aldehydes and acids. The peak at 1590 cm^{-1} was assigned to the cyclic alkenes $C = C$ stretching. Aromatic amines having $C - N$ vibration, $S = O$ stretching, and $O - H$ bending of phenol groups were affirmed by the peak around 1317 cm^{-1}, whereas the peaks between 1000 and 1200 cm^{-1} were related to $C - O$ bonds.

The XPS provides detailed information including the chemical composition, surface properties, and electronic configuration of the CDs. The XPS of C, N, O, and S are exhibited in **Fig. 3**. The peaks at 284.9, 399, 178, and 530 eV were attributed to C1s, N1s, S2p, and O1s functional groups respectively, and the atomic ratios (%) of the O, N, and C are 25.95, 1, and 73.02 as calculated from the full XPS survey. The high-resolution C1s spectra were deconvoluted into three component peaks at the binding energies of 284.9 eV ($C - C$), 285.8 eV ($C - N$, $C - O$, $C - S$), and 288.9 eV ($C = O$) assigned to adventitious carbon species (**Fig. 3**A). The XPS spectrum of O1s exhibited four predominant peaks at the binding energies 530.9 eV, 531.8 eV, 532.7 eV, and 533.2 eV, which were associated with oxygen in the states of $C - O - C$, $C = O$, $C - OH$, and $C - O$ ($N = O$), respectively (**Fig. 3**B). The high-resolution spectra of the N1s are depicted in **Fig. 3**C and the existence of the peaks at the binding energies 399.4 eV, 400.3 eV, and 401.5 eV corresponded to the presence of $N - H, N - C_3$, and $C - N - C$ configuration states [**48**]. The two peaks located at the binding energies of 168.38 eV and 169.50 eV shown in **Fig. 3**D were corresponding to S2p $_{3/2}$ and S2p $_{1/2}$ electrons, respectively, indicating the presence of the free SO_4^{-2} and SO_3^{-2} functional groups [**49, 50**].

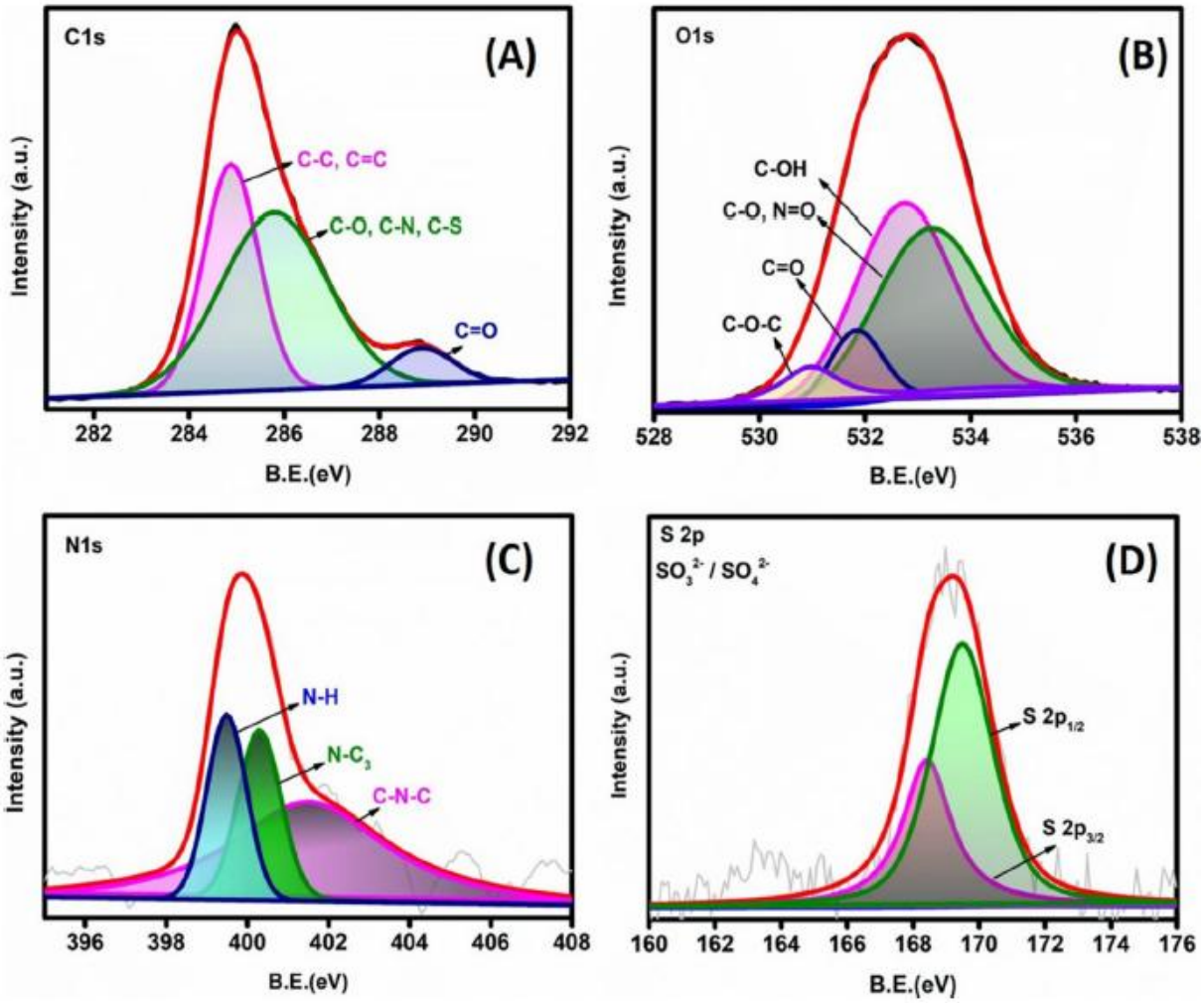

Fig. 3 XPS spectrum of biomass-derived CDs, **A** C1s spectrum; **B** O1s spectrum; **C** N1s spectrum; D S 2p spectrum

The ultrasonication coating process used ultrasonic waves to coat the CDs on the cotton textile. As shown in **Fig. 4**A, the surface morphology of the pure cotton was smooth without any disruptions.

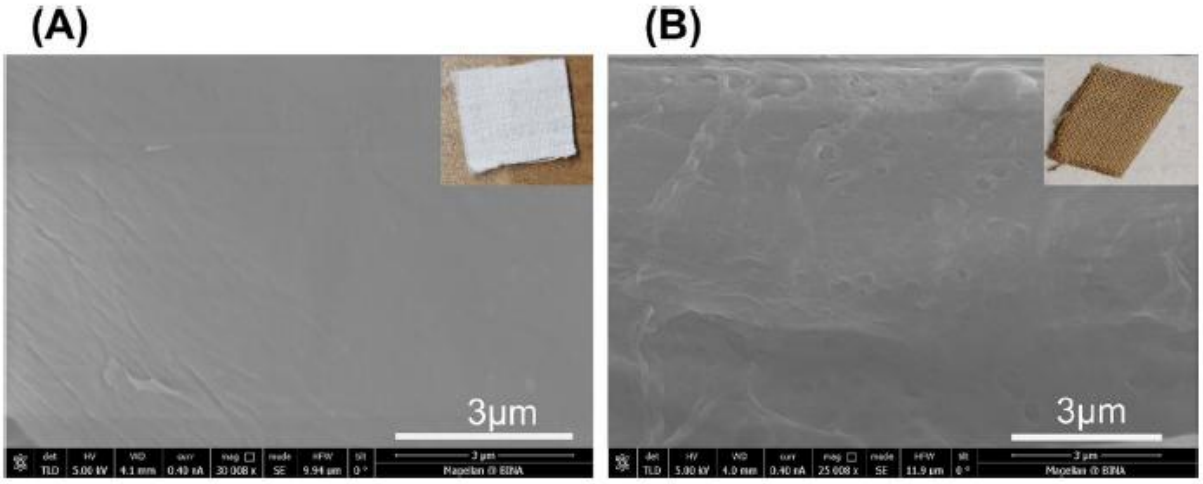

However, the disruptions due to ultrasonic waves and the cavitation ultrasonic force used to embed the CDs on the fabric can be seen in **Fig. 4**B. The breaches on the fabric surface were attributed to the incorporation of CDs into the fabric by ultrasonica-tion and the CDs might be entrapped in the intermolecular spaces of the cotton textile [**51**]. The SEM micrograph was slightly not clear due to the beam charging effect.

Fig. 4 SEM image of **A** uncoated cotton fabric, **B** carbon dot-coated fabric

3.1 Applications

3.1.1 Antibacterial aktivity

The antibacterial experiments were conducted by various concentrations of CDs within 24 h of the incubation period. This experiment demonstrates the minimum inhibitory concentration (MIC) against the bacteria which was determined to be 500 μg of CDs in 0.250 mL of an aqueous solution. This low concertation level was used for the complete eradication of all four bacteria. The eradication effect of CDs against SA and SE was effective in 12 h (**Fig. 5**B and C) and the growth inhibition was completely controlled at 12 h. For EC and KP, the effect of CDs on bacterial growth was observed after 12 h with a complete eradication at 24 h (**Fig. 5**A and D). The antibacterial tests on agar plates for EC, SA, SE, and KP are provided in **Figs. 6** and **7**.

The antimicrobial activities of the synthesized CDs were compared with other hetero-doped CDs and CDs composites [**8, 49**]. As-synthesized CDs show comparable or better antimicrobial effects without any additional chemical reagents, compounds, and passivated atoms (**Table 1**). The comparison shown in **Table 1** is based on the required incubation time and MIC/ZOI to completely eradicate the growth of different bacteria.

3.1.2 Antibacterial activity on CDs-coated fabric

The antibacterial effect of CDs-coated fabric was tested against EC, SA, SE, and KP. The uncoated fabric displayed normal cell growths for EC, SA, SE, and KP as expected. In contrast, no cell growth on the coated fabric was observed for EC, SA, and SE. For KP, only 40% of growth inhibition was observed, indicating the requirement for higher CDs loading on the fabric (**Fig. 8**). **Figure 9** indicates a

series of experiments with agar plates performed to assess the antimicrobial effect of the CDs-coated fabric against the four tested pathogens.

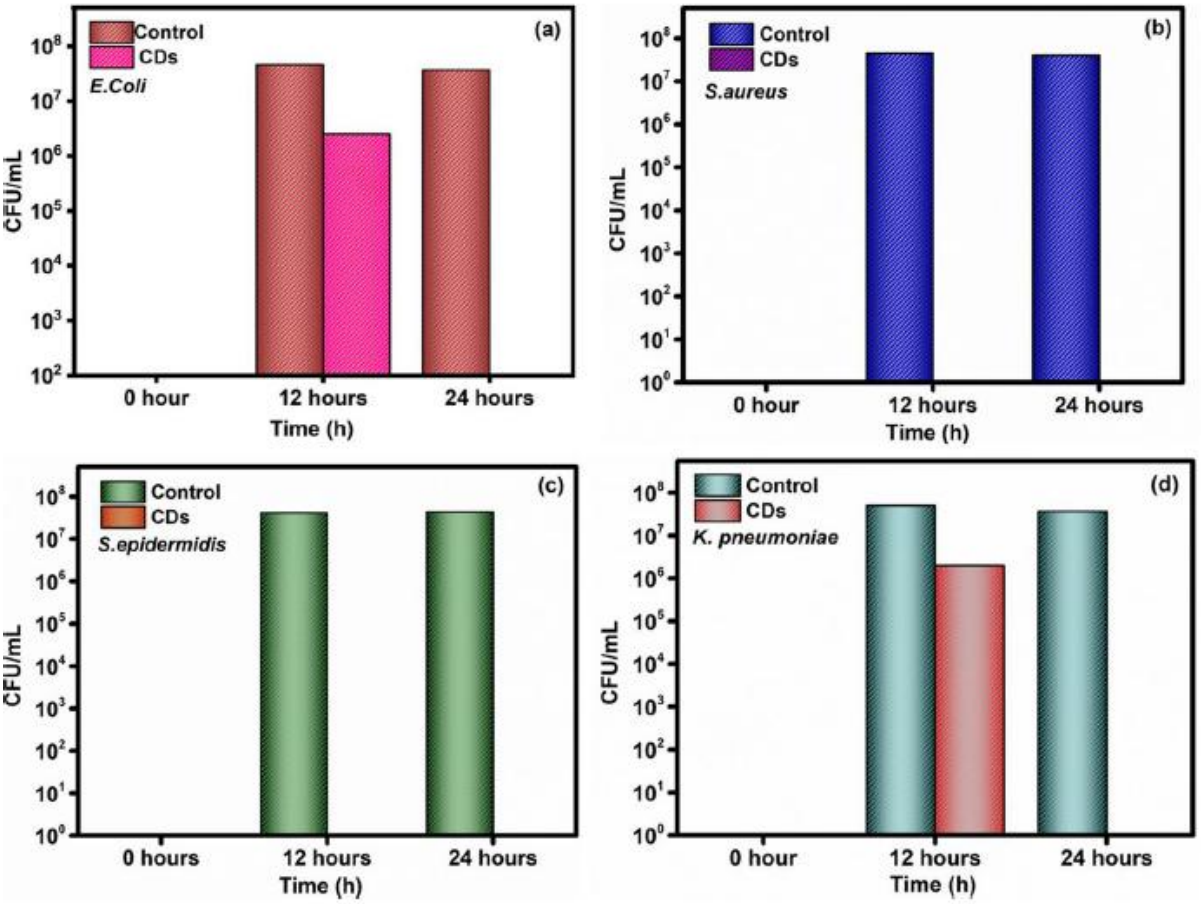

Fig. 5 The antibacterial activity of CDs, **A** CDs against EC, **B** SA, **C** SE, and **D** KP

3.2 A proposed antibacterial mechanism

It is generally accepted that CDs kill bacteria by cell wall/ membrane disruption, reactive oxygen species (ROS) generation, and DNA damage [**5**]. Gram-negative bacteria are surrounded by a thin peptidoglycan cell wall and an outer lipopolysaccharide membrane, which is highly hydrophobic. The binding of CDs to bacteria is somewhat intriguing as the positive, negative, or neutral CDs also exhibit antibacterial activities. The zeta potential of the prepared CDs with the free SO_4^{2-} and SO_3^{2-} functional groups was estimated to be - 16 mV as shown in **Fig. 10**A. However, since the bacterial cell membrane should carry a negative charge at physiological pH, the electrostatic interaction of negatively charged CDs with bacteria is not anticipated. In this context, hydrophobic interactions are envisioned between the hydrophobic domains of CDs with bacterial membrane lipids. Owing to the structure and composition difference of the bacterial surfaces of Gram-positive and Gram-negative bacteria, CDs interact with these two types of bacteria differently [**24**]. There is a significant difference in the hydrophobicity of the two types of bacteria as Grampositive bacteria have less complicated cell wall/mem-brane structures, compared to Gram-negative bacteria [**28**]. Therefore, Gram-positive bacteria are much more sensitive to lipophilic molecules than Gram-negative ones [**10**]. CDs with hydroxyl groups can also form hydrogen bonds with accessible groups of lipopolysaccharide (Gram-negative) or peptidoglycan (Gram-positive).

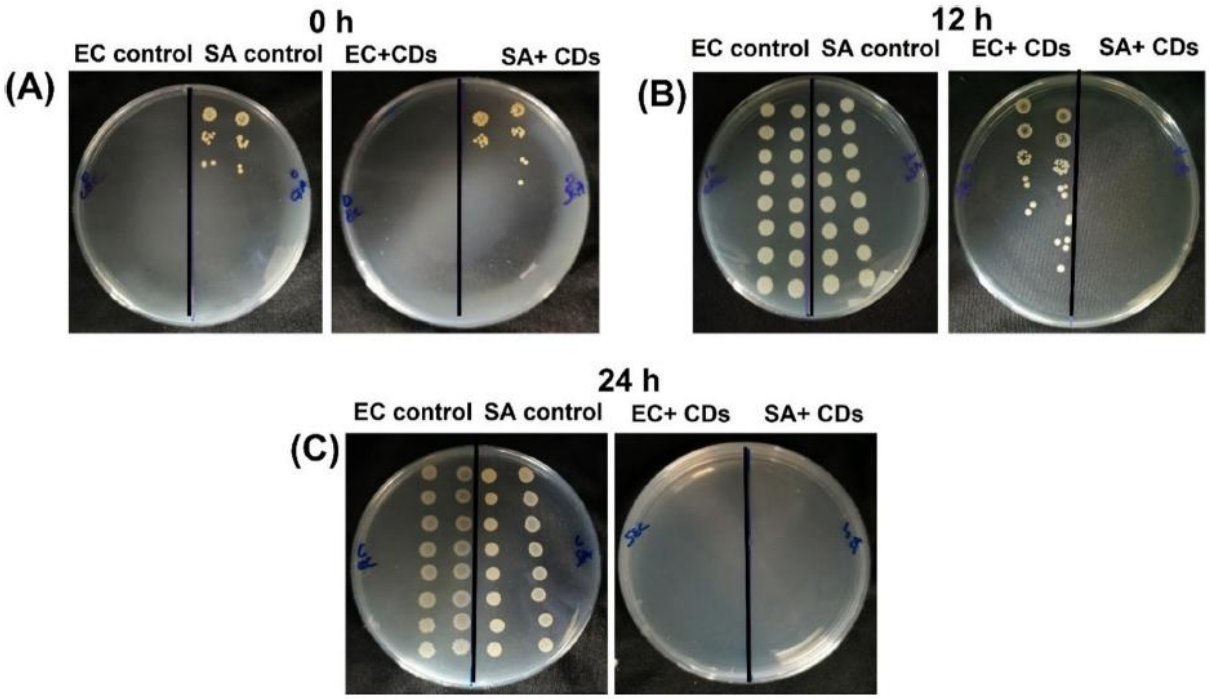

Fig. 6 Agar well plates of EC and SA at **A** 0 h with and without CDs, **B** 12 h with and without CDs, **C** 24 h with and without CDs

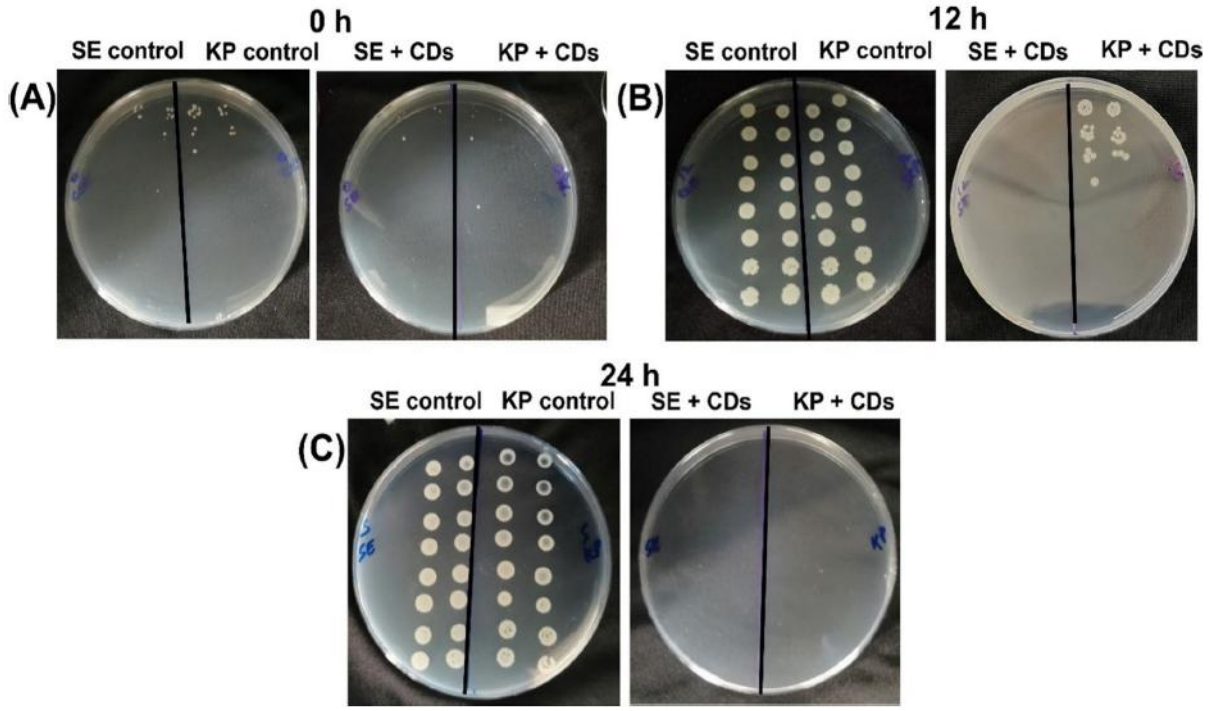

Fig. 7 Agar well plates of SE and KP at **A** 0 h with and without CDs, **B** 12 h with and without CDs, **C** 24 h with and without CDs

Table 1 Comparison of antibacterial activity with previous reports

Source	Method	Material	Bacteria	Time (h)	MIC/ZOI	Refs.
L. inermis leaves	H	CDs	EC & SA	24	5000 µg/mL	[52]
Milk vetch and tea leaves	H	OCDs TCDs	EC & SA	4	1000 µg/mL	[53]
Citric acid monohydrate	M	A-CD	EC & SA	18–24	2.5 mg/mL	[27]
m-Aminophenol and tartaric acid	H	CDs	EC & SA	24	No detection 250 µg/mL	[54]
m-Aminophenol and phosphoric acid	H	PCQD	EC & SA	12	1.23 mg/mL 1.44 mg/mL	[29]
Aminoguanidine and citric acid	H	AG/CA-CD	EC-K12 & SA	24	> 1000 mg/mL	[55]
Spermine	R	SC-Dots	EC	12	300 µg/mL	[56]
D-Glucose, diethylenetriamine	H	NCQDs	SE	18	0.5 mg/mL	[57]
Chlorhexidine gluconate	H	CDs	EC & SA	24	150 µg/mL	[58]
SCL seeds	H	CDs	EC, SA, SE, & KP	0, 12, & 24	500 µg/mL	This work

H, hydrothermal; M microwave; R, reflux

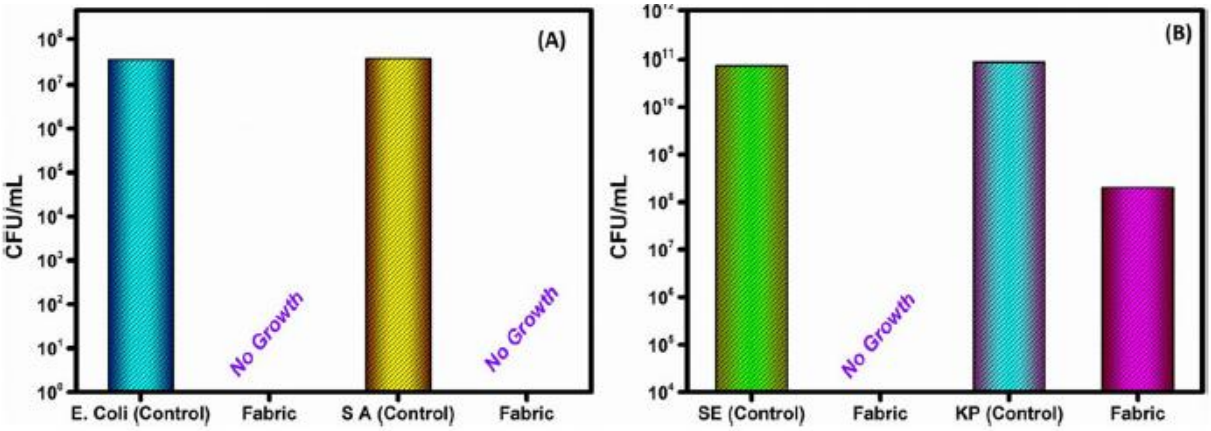

Fig. 8 Antimicrobial activities of the pristine cotton and CDs-decorated cotton on **A** EC, SA and **B** SE, KP

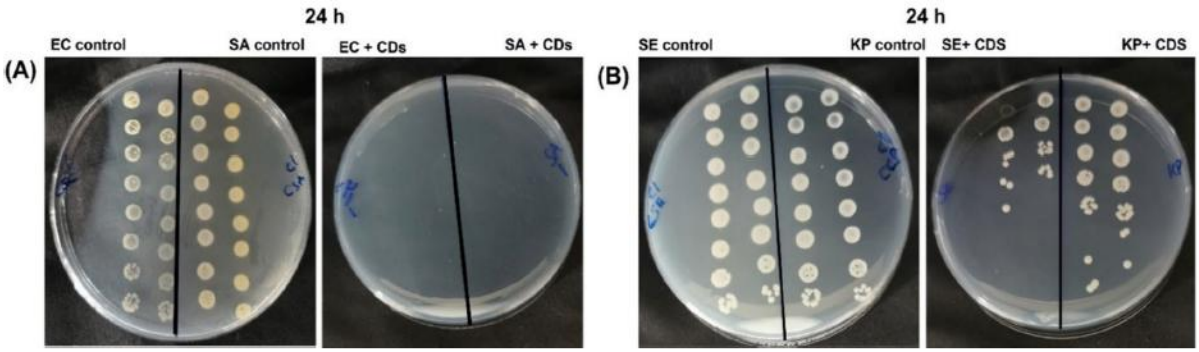

Fig. 9 A Agar well plates of EC and SA and **B** agar well plates of SE and KP at 24 h with and without coated CDs on cotton

After the binding interaction, the lone pair of electrons on the CDs eradicates bacterial cell walls [**31**], CDs produce reactive oxygen species (ROS) such as singlet oxygen (O_2), H_2O_2, hydroxyl radical ($^{\cdot}OH$), and superoxide (O_2^-), whereas NO and peroxynitrite ($ONOO^-$) are stemmed from $N@CDs$ (**Fig. 10**B). The reactive species will adhere and then penetrate the microbial cell wall to provoke oxidative stress and DNA/RNA fragmentation, resulting in corruption or inhibition of the gene expression. The reactive species also cause mitochondrial dysfunction, inactivation of intracellular protein inactivation, and lipid peroxidation, resulting in eventual cell death. The induction of oxidative stress with damages

to $DNA/\,RNA$, leading to the alterations or inhibitions of important gene expressions, and the induction of oxidative damages to proteins and other intracellular biomolecules [**59-61**].

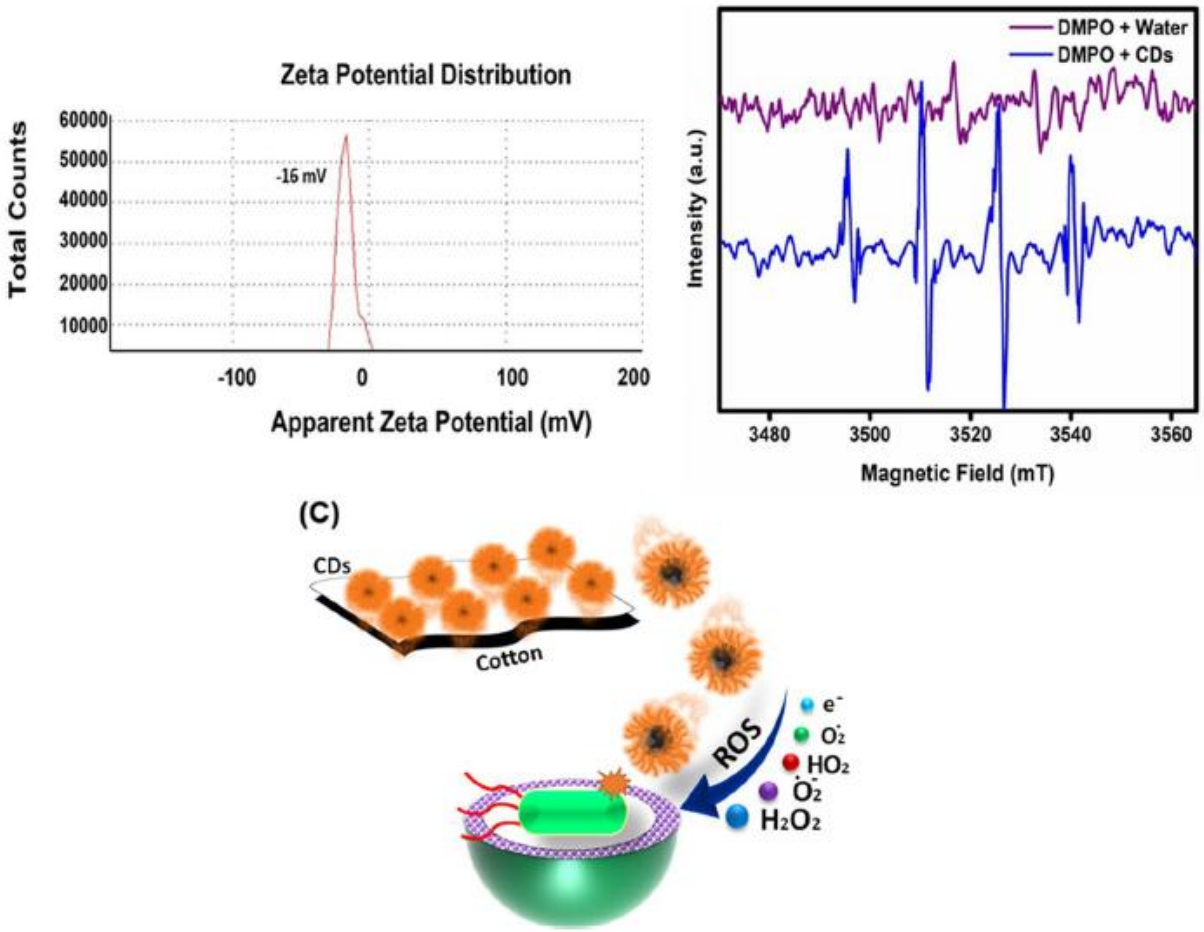

Fig. 10 A Zeta potential of CDs, **B** ESR spectra, and **C** a schematic illustration of ROS destroying the membrane

The presence of nitrogen in the synthesized CDs also participates in bacterial eradication as amine and amides of N-doped CDs play a vast role in enhancing bactericidal properties. CDs with a zeta (Z) potential - 11.06 effectively eradicate $MRSA$ [**62**]. The binding of CDs to pristine cotton deserves a brief discussion here as negatively charged CDs bind strongly to cation-ized cotton via electrostatic interaction [**63**]. As a linear-chain carbohydrate polymer with the repeated connection of D-glu-cose building blocks, cellulose carries numerous hydroxyl groups. Therefore, CDs with surface hydroxyl groups can also bind to pristine cotton via hydrogen bonds with the accessible hydroxyl groups of cellulosic building units [**64, 65**] to form a complex. While mechanistic details on the generation of ROS by different types of CDs and their corresponding antibacterial activities are still unclearly understood, the experimental results obtained in this work have shown great promise for CDs as a new class of effective antibacterial agents (**Fig. 10**C).

Among four reactive oxygen species, H_2O_2, about 3%, has been used as an antiseptic since the 1920s because it kills bacteria cells by destroying their cell walls. H_2O_2 is fairly stable while the half-life of other ROS is very short: 10^{-6} s or 1 μs for both dioxygen (singlet) or dioxidene ($^1O_2$) and superoxide anion ($O_2^{\bullet-}$) and only 10^{-9} s or 1 ns for hydroxyl radicals ($HO^{\bullet}$) [**66**]. ROS are natural byproducts of cellular oxidative metabolism and play important roles in the modulation of cell survival, cell death, differentiation, cell signaling, and inflammation-related factor production [**67, 68**].

These low concentrations of ROS enable their role as second messengers in signal transduction for vascular homeostasis and cell signaling. Under normal circumstances, ROS concentrations are tightly controlled by antioxidants, keeping them in the picomolar range [**69**]. When excessively produced, or when antioxidants are depleted, ROS can inflict damage on lipids, proteins, and DNA. CDs are generally safe as confirmed by cytotoxicity assays for various cell limes; however, small changes in the synthesis conditions can have significant effects on the properties of CDs [**70**]. Nonetheless, in vivo safety analyses of CDs remain unclear, which is worthy of future evaluation.

4 Conclusion

CDs with antimicrobial properties were successfully synthesized from SCL seed extract by one-pot hydrothermal synthesis. The production of reactive oxygen species was postulated to play an important role in the bacterial eradication of both Gram-positive and Gram-negative bacteria. The antibacterial application was taken one step forward by coating cotton textiles with CDs by ultrasonication. The process yielded a good coating of CDs on the cotton without the use of any additional or toxic chemicals. Albeit an exact mechanism of microbial activities of CDs decorated cotton is a subject of future endeavor, this study suggests a potential fabrication of textiles with excellent microbicide activity.

References

1. Liang J, Li W, Chen J et al (2021) Antibacterial activity and synergetic mechanism of carbon dots against gram-positive and -negative bacteria. ACS Appl Bio Mater 4:6937-6945. **https://doi.org/ 10.1021/ACSABM. 1C00618/ASSET/IM AGES/LARGE/MT1C0 0618_0007.JPEG**

2. Dong X, Liang W, Meziani MJ et al (2020) Carbon dots as potent antimicrobial agents. Theranostics 10:671. **https://doi.org/10. 7150/THNO.39863**

3. Ghafoor D, Khan Z, Khan A et al (2021) Excessive use of disinfectants against COVID-19 posing a potential threat to living beings. Curr Res Toxicol 2:159-168. **https://doi.org/10.1016/J. CRTOX.2021.02.008**

4. Linklater DP, De Volder M, Baulin VA et al (2018) High aspect ratio nanostructures kill bacteria via storage and release of mechanical energy. ACS Nano 12:6657-6667. **https://doi.org/10. 1021/ACSNANO.8B01665/SUPPL_FILE/NN8B01665_SI_002. AVI**

5. Lin F, Wang Z, Wu FG (2022) Carbon dots for killing microorganisms: an update since 2019. Pharm 15(1236 15):1236. **https://doi. org/10.3390/PH15101236**

6. Marković ZM, Matijašević DM, Pavlović VB et al (2017) Antibacterial potential of electrochemically exfoliated graphene sheets. J Colloid Interface Sci 500:30-43. **https://doi.org/10. 1016/J.JCIS.2017.03.110**

7. Zheng H, Ma R, Gao M et al (2018) Antibacterial applications of graphene oxides: structure-activity relationships, molecular initiating events and biosafety. Sci Bull 63:133-142. **https://doi. org/10.1016/J.SCIB.2017.12.012**

8. Chen H, Wang B, Zhao R et al (2015) Coculture with low-dose SWCNT attenuates bacterial invasion and inflammation in human enterocyte-like Caco-2 cells. Small 11:4366-4378. **https ://doi.org/10.1002/SMLL.201500136**

9. Chai S, Zhou L, Pei S et al (2021) P-doped carbon quantum dots with antibacterial activity. Micromachines 12:1116. **https ://doi. org/10.33 90/MI12091116**

10. Yang J, Zhang X, Ma YH et al (2016) Carbon dot-based platform for simultaneous bacterial distinguishment and antibacterial applications. ACS Appl Mater Interfaces 8:32170-32181. **https://doi.org/10.1021/ACSAMI.6B10398/ASSET/IMAGES/ LARGE/AM-2016-103 98 3_0007. JPEG**

11. Cui L, Ren X, Sun M et al (2021) Carbon dots: synthesis, properties and applications. Nanomater. 11:3419. **https://doi.org/10. 3390/NANO11123419**

12. Xu X, Ray R, Gu Y et al (2004) Electrophoretic analysis and purification of fluorescent single-walled carbon nanotube fragments. J Am Chem Soc 126:12736-12737. **https://doi.org/10. 1021/JA040082H/SUPPL_FILE/JA040082H_S.PDF**

13. Ghirardello M, Ramos-Soriano J, Galan MC (2021) Carbon dots as an emergent class of antimicrobial agents. Nanomater 11:1877. **https://doi.org/10.3390/NANO11081877**

14. Reyes D, Camacho M, Camacho M et al (2016) Laser ablated carbon nanodots for light emission. Nanoscale Res Lett 11:111. **https://doi.org/10.1186/S11671-016-1638-8/FIGURES/9**

15. Chao-Mujica FJ, Garcia-Hernández L, Camacho-López S et al (2021) Carbon quantum dots by submerged arc discharge in water: synthesis, characterization, and mechanism of formation. J Appl Phys. 129:163301. **https://doi.org/10.1063Z5.0040322**

16. Han Z, He L, Pan S et al (2020) Hydrothermal synthesis of carbon dots and their application for detection of chlorogenic acid. Luminescence 35:989-997. **https://doi.org/10.1002/BIO. 3803**

17. De Medeiros TV, Manioudakis J, Noun F et al (2019) Microwave-assisted synthesis of carbon dots and their applications. J Mater Chem C 7:7175-7195. **https://doi.org/10.1039/C9TC01640F**

18. Jorns M, Pappas D, Tagmatarchis N, Kelarakis A (2021) A review of fluorescent carbon dots, their synthesis, physical and chemical characteristics, and applications. Nanomater 11:1448. **https://doi. org/10.3390/NANO11061448**

19. Bhamore JR, Jha S, Park TJ, Kailasa SK (2019) Green synthesis of multi-color emissive carbon dots from Manilkara zapota fruits for bioimaging of bacterial and fungal cells. J Photochem Photobiol B Biol 191:150-155. **https://doi.org/10.1016/JJPHOTOBIOL.2018. 12.023**

20. Zulfajri M, Abdelhamid HN, Sudewi S et al (2020) Plant part-derived carbon dots for biosensing. Biosens 10:68. **https://doi. org/10.3390/BIOS10060068**

21. Peng Z, Ji C, Zhou Y et al (2020) Polyethylene glycol (PEG) derived carbon dots: preparation and applications. Appl Mater Today. 20:100677. **https://doi.org/10.1016/J.APMT.2020.100677**

22. Qureashi A, Pandith AH, Bashir A, Malik LA (2021) Biomass-derived carbon quantum dots: a novel and sustainable fluorescent “ON-OFF-ON” sensor for ferric ions. Anal Methods 13:47564766. **https://doi.org/10.1039/D1AY01112J**

23. Ren J, Malfatti L , Innocenzi P (2020) Citric acid derived carbon dots, the challenge of understanding the synthesis-structure relationship. C. 7:2. **https://doi.org/10.3390/C7010002**

24. Yang J, Gao G, Zhang X et al (2019) One-step synthesis of carbon dots with bacterial contact-enhanced fluorescence emission: fast gram-type identification and selective Gram-positive bacterial inactivation. Carbon N Y 146:827-839. **https://doi.org/10.1016/J. CARBON.2019.02.040**

25. Anand A, Unnikrishnan B, Wei SC et al (2018) Graphene oxide and carbon dots as broad-spectrum antimicrobial agents - a minireview. Nanoscale Horizons 4:117-137. **https://doi.org/10.1039/ C8NH00174J**

26. Bing W, Sun H, Yan Z et al (2016) Programmed bacteria death induced by carbon dots with different surface charge. Small 12:4713-4718. **https://doi.org/10.1002/SMLL.201600294**

27. Sahiner N, Suner SS, Sahiner M, Silan C (2019) Nitrogen and sulfur doped carbon dots from amino acids for potential biomedical applications. J Fluoresc 29:1191-1200. **https://doi.org/10.1007/ S10895-019-02431 -Y/TABLES/2**

28. Ran HH, Cheng X, Bao YW et al (2019) Multifunctional quater-nized carbon dots with enhanced biofilm penetration and eradication efficiencies. J Mater Chem B 7:5104-5114. **https://doi.org/ 10.1039/C9TB00681H**

29. Elango D, Packialakshmi JS, Manikandan V, Jayanthi P (2022) Sustainable synthesis of carbon quantum dots from shrimp shell and its emerging applications. Mater Lett. 312:131667. **https:// doi.org/10.1016/J.MATLET.2022.131667**

30. Raina S, Thakur A, Sharma A et al (2020) Bactericidal activity of Cannabis sativa phytochemicals from leaf extract and their derived carbon dots and Ag@carbon dots. Mater Lett. 262:127122. **https:// doi. or g/10.1016/J. M ATLET.2019.127122**

31. Saravanan A, Maruthapandi M, Das P et al (2021) Green synthesis of multifunctional carbon dots with antibacterial activities. Nanomater 11:369. **https://doi.org/10.3390/NANO11020369**

32. Eskalen H, Çeşme M, Kerli S, Őzgan § (2021) Green synthesis of water-soluble fluorescent carbon dots from rosemary leaves: applications in food storage capacity, fingerprint detection, and antibacterial activity. J Chem Res 45:428-435. **https://doi.org/10. 1177/1747519820953823/ASSET/IMAGES/LARGE/10.1177_ 1747519820953823-FIG1. JPEG**

33. Kadiyala NK, Mandal BK, Ranjan S, Dasgupta N (2018) Bioinspired gold nanoparticles decorated reduced graphene oxide nanocomposite using Syzygium cumini seed extract: evaluation of its biological applications. Mater Sci Eng C 93:191-205. **https://doi. org/10.1016/J.MSEC.2018.07.075**

34. Saravanan A, Maruthapandi M, Das P et al (2020) Applications of N-doped carbon dots as antimicrobial agents, antibiotic carriers, and selective fluorescent probes for nitro explosives. ACS Appl Bio Mater 3:8023-8031. **https://doi.org/10.1021/ACSABM. 0C01104/ASSET/IMAGES/LARGE/MT0C01104_0007.JPEG**

35. Maruthapandi M, Saravanan A, Manohar P et al (2021) Photocatalytic degradation of organic dyes and antimicrobial activities by polyaniline-nitrogen-doped carbon dot nanocomposite. Nanomater 11:1128. **https://doi.org/10.3390/NANO11051128**

36 Maruthapandi M, Das P, Saravanan A et al (2021) Biocompatible N-doped carbon dots for the eradication of methicillin-resistant S. aureus (MRSA) and sensitive analysis for europium (III). NanoStructures Nano-Objects. 26:100724. **https://doi.org/10.1016/J. NANOSO.2021.100724**

37. Malka E, Perelshtein I, Lipovsky A et al (2013) Eradication of multi-drug resistant bacteria by a novel Zn-doped CuO nanocomposite. Small 9:4069-4076. **https://doi.org/10.1002/SMLL.20130 1081**

38. Perkas N, Amirian G, Dubinsky S et al (2007) Ultrasound-assisted coating of nylon 6,6 with silver nanoparticles and its antibacterial activity. J Appl Polym Sci 104:1423-1430. **https://doi.org/10. 1002/APP.24728**

39. Perelshtein I, Ruderman Y, Perkas N et al (2013) The sonochemi-cal coating of cotton withstands 65 washing cycles at hospital washing standards and retains its antibacterial properties. Cellulose 20:1215-1221. **https://doi.org/10.1007/S10570-013-9929-Z/ FIGURES/6**

40. Maruthapandi M, Saravanan A, Manoj S et al (2021) Facile ultrasonic preparation of a polypyrrole membrane as an absorbent for efficient oil-water separation and as an antimicrobial agent. Ultrason Sonochem. 78:105746. **https://doi.org/10.1016/JZULTSONCH.2021.105746**

41. Sanchez Ramirez DO, Varesano A, Carletto RA et al (2019) Antibacterial properties of polypyrrole-treated fabrics by ultrasound deposition. Mater Sci Eng C 102:164-170. **https://doi.org/10. 1016/J.MSEC.2019.04.016**

42. Javed N, O'Carroll DM (2021) Carbon dots and stability of their optical properties. Part Part Syst Charact 38:2000271. **https://doi. org/10.1002/PPSC.202000271**

43. Ansi VA, Renuka NK (2018) Table sugar derived carbon dot - a naked eye sensor for toxic Pb2+ ions. Sensors Actuators B Chem 264:67-75. **https://doi.org/10.1016ZJ.SNB.2018.02.167**

44. Ding H, Wei J-S, Zhang P et al (2018) Solvent-controlled synthesis of highly luminescent carbon dots with a wide color gamut and narrowed emission peak widths. Small 14:1800612. **https://doi.org/10.1002/SMLL.201800612**

45. Ding H, Yu SB, Wei JS, Xiong HM (2016) Full-color light-emitting carbon dots with a surface-state-controlled luminescence mechanism. ACS Nano 10:484-491. **https://doi.org/10.1021/ACSNANO.5B05406/ASSET/IMAGES/LARGE/NN-2015-054069_0007.JPEG**

46. Reckmeier CJ, Schneider J, Xiong Y et al (2017) Aggregated molecular fluorophores in the ammonothermal synthesis of carbon dots. Chem Mater 29:10352-10361. **https://doi.org/10.1021/ACS.CHEMMATER.7B03344/ASSET/IMAGES/LARGE/CM-2017-03344P_0005.JPEG**

47. Ayyanar M, Subash-Babu P (2012) Syzygium cumini (L.) Skeels: a review of its phytochemical constituents and traditional uses. Asian Pac J Trop Biomed 2:240-246. **https://doi.org/10.1016/ S2221-1691(12)60050-1**

48. Li H, Xie Y, Liu Y et al (2021) Surface chemical functionality of carbon dots: influence on the structure and energy storage performance of the layered double hydroxide. RSC Adv 11:1078510793. **https://doi.org/10.1039/D1RA00706H**

49. Maruthapandi M, Saravanan A, Luong JHT, Gedanken A (2022) Polydopamine decorated carbon dots nanocomposite as an effective adsorbent for phenolic compounds. J Appl Polym Sci 139:51769. **https ://doi.org/10.1002/APP. 51769**

50. Tresintsi S, Simeonidis K, Pliatsikas N et al (2014) The role of SO42- surface distribution in arsenic removal by iron oxy-hydroxides. J Solid State Chem 213:145-151. **https://doi.org/10. 1016/J. JSSC.2014.02.026**

51. Ahmed HB, Abualnaja KM, Ghareeb RY et al (2021) Technical textiles modified with immobilized carbon dots synthesized with infrared assistance. J Colloid Interface Sci 604:15-29. **https://doi. org/10.1016/J. JCIS.2021.07.014**

52. Shahshahanipour M, Rezaei B, Ensafi AA, Etemadifar Z (2019) An ancient plant for the synthesis of a novel carbon dot and its applications as an antibacterial agent and probe for sensing of an anti-cancer drug. Mater Sci Eng C 98:826-833. https://doi.org/ 10.1016/J.MSEC.2019.01.041

53. Ma Y, Zhang M, Wang H et al (2020) N-doped carbon dots derived from leaves with low toxicity via damaging cytomem-brane for broad-spectrum antibacterial activity. Mater Today Commun. 24:101222. **https://doi.org/10.10167r.MTCOMM.2020. 1**01222

54. Wang H, Lu F, Ma C et al (2021) Carbon dots with positive surface charge from tartaric acid and m -aminophenol for selective killing of Gram-positive bacteria. J Mater Chem B 9:125-130. **https://doi.org/10.1039/D0TB02332A**

55. Otis G, Bhattacharya S, Malka O et al (2019) Selective labeling and growth inhibition of Pseudomonas aeruginosa by aminoguani-dine carbon dots. ACS Infect Dis 5:292-302. **https://doi.org/10.1021/ACSINFECDIS.8B00270/ASSET/IMAGES/LARGE/ID-2018-00270B_0009.JPEG**

56. Li P, Sun L, Xue S et al (2022) Recent advances of carbon dots as new antimicrobial agents. SmartMat 3:226-248. **https://doi.org/ 10.1002/SMM2.1131**

57. Zhao C, Wang X, Wu L et al (2019) Nitrogen-doped carbon quantum dots as an antimicrobial agent against Staphylococcus for the treatment of infected wounds. Colloids Surfaces B Biointerfaces 179:17-27. **https://doi.org/10.1016/J.COLSURFB.2019.03.042**

58. Sun B, Wu F, Zhang Q et al (2021) Insight into the effect of particle size distribution differences on the antibacterial activity of carbon dots. J Colloid Interface Sci 584:505-519. **https://doi.org/ 10.1016/J.JCIS.2020.10.015**

59. Al Awak MM, Wang P, Wang SY, Tang YA, Sun YP, Yang LJ (2017) Correlation of carbon dots' light-activated antimicrobial activities and fluorescence quantum yield. RSC Adv 7:30177-30184

60. Li H, Huang J, Song YX, Zhang ML, Wang HB, Lu F et al (2018) Degradable carbon dots with broad-spectrum antibacterial activity. ACS Appl Mater Inter 10:26936-26946

61. Li YJ, Harroun SG, Su YC, Huang CF, Unnikrishnan B, Lin HJ et al (2016) Synthesis of self-assembled spermidine-carbon quantum dots effective against multidrug-resistant bacteria. Adv Healthc Mater 5:2545-2554

62. Kung JC, Tseng IT, Chien CS et al (2020) Microwave assisted synthesis of negative-charge carbon dots with potential antibacterial activity against multi-drug resistant bacteria. RSC Adv 10:41202-41208. **https://doi.org/10.1039/D0RA07106D**

63. Emam HE, El-Shahat M, Hasanin MS, Ahmed HB (2021) Potential military cotton textiles composed of carbon quantum dots clustered from 4-(2,4-dichlorophenyl)-6-oxo-2-thioxohexahy-dropyrimidine-5-carbonitrile. Cellulose 28:9991-10011. **https:// doi.org/10.1007/S10570-021 -04147-4/TABLES/5**

64. Emam HE, Abdellatif FHH, Abdelhameed RM (2018) Cationi-zation of celluloisc fibers in respect of liquid fuel purification. J Clean Prod 178:457-467. **https://doi.org/10.1016/JJCLEPRO. 2018.01.048**

65. Li W, Zhang H, Zheng Y et al (2017) Multifunctional carbon dots for highly luminescent orange-emissive cellulose based composite phosphor construction and plant tissue imaging. Nanoscale 9:12976-12983. **https://doi.org/10.1039/C7NR0 3217J**

66. Taverne YJ, Bogers AJ, Duncker DJ, Merkus D (2013) Reactive oxygen species and the cardiovascular system. Oxid Med Cell Longev 2013:862423

67. Mueller CF, Laude K, McNally JS, Harrison DG (2005) Redox mechanisms in blood vessels. Arterioscler Thromb Vasc Biol 25:274-278

68. Touyz RM (2013) Molecular and cellular mechanisms in vascular injury in hypertension: role of angiotensin II-editorial review. Curr Opin Nephrol Hypertens 14:125-131

69. Droge W (2002) Free radicals in the physiological control of cell function. Physiol Rev 82(1):47-95

70. Esfandiari N, Bagheri Z, Ehtesabi H, Fatahi Z, Tavana H, Latifi H (2019) Effect of carbonization degree of carbon dots on cytotoxicity and photo-induced toxicity to cells. Heliyon 5(12):e02940